journal

J. Am. Ceram. Soc., 95 [10] 3144–3150 (2012)
DOI: 10.1111/j.1551-2916.2012.05418.x

Sintering, Crystallization, and Dielectric Behavior of Barium Zinc Borosilicate Glasses—Effect of Barium Oxide Substitution for Zinc Oxide

Regina C. C. Monteiro,[‡,†] Andreia A. S. Lopes,[‡] Maria M. A. Lima,[‡] João P. Veiga,[‡] Rui J. C. Silva,[‡] Carlos J. Dias,[‡] Erika J. R. Davim,[§] and Maria H. V. Fernandes[§]

[‡]CENIMAT/I3N, Department of Materials Science, Faculty of Sciences and Technology, Universidade Nova de Lisboa, Caparica 2829-516, Portugal

[§]CICECO and Department of Ceramics and Glass Engineering, University of Aveiro, Campus Universitário de Santiago, Aveiro 3810-193, Portugal

Barium zinc borosilicate glasses with a molar composition xBaO-(60−x)ZnO-30B_2O_3-10SiO_2, where x ranged from 0 to 60 mol%, were prepared using melt-quenching method. The effect of BaO substitution for ZnO on the sintering, crystallization, and dielectric characteristics has been investigated. The behavior of the studied barium zinc borosilicate glasses was mainly determined by the relative amount of the structural modifier oxides (BaO and ZnO) and the ionic size, and field strength of the modifying cations (Ba^{2+}, Zn^{2+}). Increased amounts of BaO decreased both glass transition temperature and crystallization temperature, while increasing the relative dielectric constant. Sintering occurred before crystallization for glasses where substitution of BaO for ZnO was up to 30 mol%, but for higher substitution levels, crystallization occurred during the sintering process hindering densification.

I. Introduction

Recent great developments in various electronic industries such as display panels, low-temperature cofired ceramics, and packaging require different types of low-temperature sinterable glasses with specific characteristics. Among these glasses, borosilicate glasses are considered promising candidates for such applications due to their low softening temperature, low dielectric constant, and high electrical resistance.[1–5] To reduce the firing temperature, some alkali or bivalent metal oxides must be added, often at the expense of dielectric properties as well as crystallization behavior.[1]

PbO containing borate glass systems, e.g., PbO–B_2O_3–SiO_2 and PbO–ZnO–B_2O_3, have become popular as commercial low-temperature sinterable glasses due to their high structural stability, low glass transition temperature, and good thermal and electrical characteristics.[6–8] However, PbO is a component with deleterious health and environmental effects during processing and therefore development of environmental-friendly materials that can replace the PbO-based glasses is of utmost importance. Recently, BaO and ZnO have been employed as potential candidate components that can replace PbO in low-temperature sinterable glasses.[2,3,9–11] In this case, to obtain glasses with low glass transition temperatures, significant amount of a glass network modifier is necessary, which almost inevitably results in the crystallization of the glass.[10,11]

Recently, the quaternary BaO–ZnO–B_2O_3–SiO_2 system, which is nonhazardous,[12] has been reported as an alternative material to PbO containing systems, and no evidence of crystallization was found when some selected glass compositions were heated at ~580°C.[13–15] BaO is a component for adjusting viscosity at high temperature, to affect the deformability of the glass, and for elevating the thermal expansion coefficient of the glass. It was reported that by controlling the glass compositions within this quaternary system, it is possible to obtain transparent glasses sintered a low temperatures, between 550°C and 580°C.[14]

During the sintering process of glass powders, where the densification is mainly due to viscous flow,[16] the crystallization of the glass may occur.[4,17,18] Glass particles tend to crystallize at the surface, and the crystallized phase alters significantly the sintering behavior and the physical characteristics of the glass.[10] If crystallization occurs at the early stages of the sintering process, that is, at temperatures very close to the glass transition temperature, the sintering of the glass will be inhibited resulting in a porous material, where the crystalline phase can grow in an uncontrollable way. Therefore, the study of the sintering process of glass powders is a very challenging task both on the scientific and technological points of view. The definition of the glass composition, sintering parameters, and temperature working window required to accomplish a fully dense glass without the occurrence of crystallization is of great practical interest.

In the present study, different glass compositions based on BaO–ZnO–B_2O_3–SiO_2(BaZBS) system were prepared and the influence of BaO/ZnO content on the sinterability of the glass frits, on the crystallization behavior, and on the dielectric properties of the glasses was investigated.

II. Experimental Procedure

For the preparation of the glasses, $BaCO_3$ (BDH), ZnO (Merck, Darmstadt, Germany), H_3BO_3(Merck), and SiO_2(BDH),with purity higher than 99%, were used as the starting materials. The amounts of $B_2O_3$and SiO_2, glass network formers, were fixed at 30 and 10 mol%, respectively, and the remaining 60 mol% was filled with BaO and ZnO, glass network modifiers. The compositions of the studied glasses are presented in Table I. Batches of 10 g were prepared by weighing the right amounts of the raw materials, mixing for 30 min in a teflon jar, using a laboratory powder mixer (turbula WAB, T2F, Muttenz, Switzerland), and melting the mixture in a Pt crucible in an electric furnace for 2 h in air. To achieve a fully homogeneous melt, compositions containing up to 30 mol% BaO were heated at 1250°C, although a temperature of 1450°C was necessary for the remaining compositions, with an higher amount of BaO. Then, the molten glass was poured into water for quenching.

L. Pinckney—contributing editor

Manuscript No. 31461. Received May 10, 2012; approved July 23, 2012.
†Author to whom correspondence should be addressed. e-mail: rcm@fct.unl.pt

Table I. Compositions of $BaO–ZnO–B_2O_3–SiO_2$ Glasses (mol%)

Designation	BaO	ZnO	B_2O_3	SiO_2
GBa0	0	60	30	10
GBa10	10	50	30	10
GBa20	20	40	30	10
GBa30	30	30	30	10
GBa40	40	20	30	10
GBa50	50	10	30	10
GBa60	60	0	30	10

The glass frit was dried, milled with absolute ethanol for 2 h in an agate ball mill (Pulverizette; Fritsch, Idar-Oberstein, Germany), dried again, and sieved to obtain a glass powder with a particle size lower than 65 μm.

The amorphous state of the glass frit was observed using X-ray diffraction (XRD) analysis performed in a DMAX-III C diffractometer (Rigaku Industrial Corporation, Tokyo, Japan) using Cu$K\alpha$ radiation (40 kV, 30mA) with a scanning rate of 2°/min and a sampling interval of 0.01° (2θ). Elemental chemical analysis of the different glass powders carried out in an X-ray fluorescence spectrometer (WDXRF, Axios; PANalytical, Almelo, Netherlands) revealed that they agree with the formulated compositions within the experimental error of 20%, max. The density of the glass powders was measured in a helium pycnometer (Accupyc 1330; Micromeritics, Norcross, GA). The glass transition temperature and crystallization temperature of the glasses were assessed using differential thermal analysis (DTA). These temperature values were determined using the software associated to the DTA equipment (STA PT1600; Linseis, Selb, Germany), and the measurement error is assumed as 1%.

Subsequently, cylindrical powder compacts (≈3 mm height, 13 mm diameter)were prepared from the different glass compositions by uniaxial pressing the powders under a compressive stress of ~75 MPa. The green density (ρ_g) of the powder compacts was determined from the mass and the geometrical dimensions, these being measured with a micrometer caliper. The compacts were sintered in an electric tubular furnace at a heating rate of 5°C/min from room temperature up to a temperature between 480°C and 620°C, as suggested by the glass DTA results, held during 1 h at the selected temperature, and then the furnace was switched off and the samples cooled inside the furnace.

To evaluate the sintering behavior of the different glass samples, the density, porosity, and linear shrinkage of the sintered samples were determined. Bulk density, apparent (open) porosity, apparent density, and closed porosity were calculated from the dry weight of the sample, the saturated weight in water and the suspended weight in water, determined according to a standard procedure (ASTM C20-83, vol.15.01, 1985). The linear shrinkage was calculated in terms of the radial shrinkage, $\Delta R/R_o = (R_o - R)/R_o$, where R_o and R are the initial and the final sample radius, respectively, and in terms of the axial shrinkage, $\Delta H/H_o = (H_o - H)/H_o$, where H_o and H are the initial and the final sample height, respectively. At least three powder compacts of each BaZBS glass composition were sintered at the selected temperature and the mean values of density, porosity, and linear shrinkage of the sintered samples were determined.

Crystallization of the sintered specimens was analyzed using XRD. The microstructure of the sintered samples was observed using a scanning electron microscope, SEM (DSM 960; Zeiss, Jena, Germany) equipped with an energy dispersive spectrometer, EDS (INCAx-sight ; Oxford Instruments, Austin, TX). The dielectric characteristics (permittivity and dielectric loss) of the sintered glass specimens were analyzed using an automatic capacitance bridge (model 2500; Andeen-Hagerling, Cleveland, OH) at room temperature, and at a frequency of 100 kHz, 500 kHz, and 1 MHz.

III. Results and Discussion

(1) Glass Powder Characterization

The X-ray diffraction patterns of different BaZBS glass powders are presented in Fig. 1. A broad peak around 2θ = 35° is observed for the composition without BaO. For glasses with a BaO content 10–30 mol%, the broad peak is around 2θ = 28°, whereas for glasses containing a higher amount of BaO, two broad peaks are clearly observed, at ~2θ = 28° and 43°, which is characteristic of borate glasses.[3,6] XRD results show that the prepared glass samples are typically in the amorphous state, although for the composition containing 60 mol% BaO, a very slight diffraction peak might be considered at ~25°, which can be attributed to the incipient formation of BaB_2O_4(25.3°, JCPDS File 38-0722). Melting at a higher temperature was not tried for that particular composition to avoid the possible volatilization of B_2O_3.[19] The tendency for crystallization of BaB_2O_4 and B_2O_3 in a glass with 60 mol% BaO, has been reported by Lim *et al.*,[6] who studied a series of glasses from the ternary system $BaO–B_2O_3–SiO_2$ (BaBS), where the amount of SiO_2 was fixed at 10 mol% and the amount of BaO and B_2O_3 totalized 90 mol%.

The change of the density (ρ) of the different prepared BaZBS glass powders with the BaO content is shown in

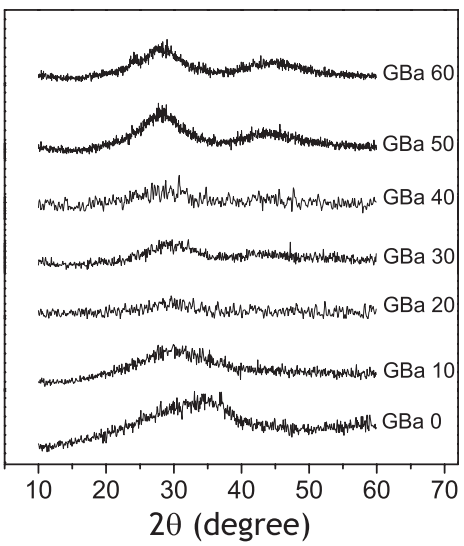

Fig. 1. X-ray diffraction patterns of glass powders.

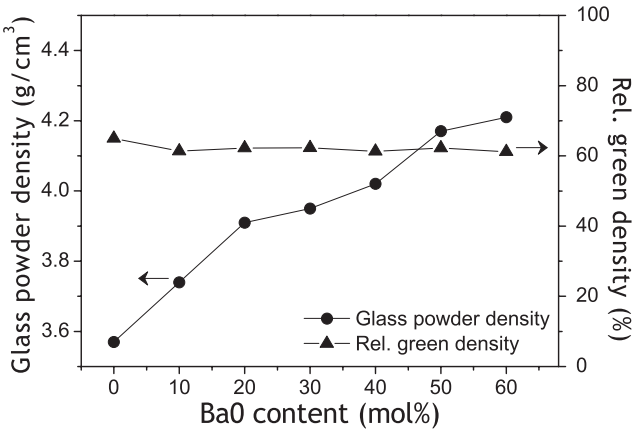

Fig. 2. Density of the glass powders and relative green density of powder compacts as a function of BaO content.

Fig. 2. The glass powder density (ρ) increases with the BaO content because the molecular weight of BaO is much higher than the molecular weight of the remaining components. It is observed that the line (shown as guide for the eye) has a first slope between 0 and 20 mol% BaO and a second slope for higher BaO content. For glasses from the ternary BaBS system with a shorter range of BaO (35–55 mol%) it was reported that the powder density varied near linearly with BaO content.[6]

For the different studied BaZBS glass compositions, the values of the green density (ρ_g) of the powder compacts to be used in the sintering process ranged between 2.32 and 2.60 g/cm^3. The relative green density of the powder compacts, determined as the ratio between the green density and density of the glass powder, is also shown in Fig. 2. The relative green density of the powder compacts was 63 ± 2 (%), meaning that before the sintering process a porosity of 37 ± 2 (%) was present. It is verified that the relative green density slightly decreases with the BaO content, suggesting that particle packaging differed for the different glass powder compositions.

Figure 3 shows the DTA curves of the BaZBS glass powders obtained at a heating rate of 10°C/min. From these data, the thermal behavior of the glasses was analysed, and the glass transition temperature (T_g), the onset crystallization temperature (T_c), and the maximum crystallization temperature (T_p) were determined. In some DTA curves, two exothermic effects can be clearly observed, and curves for glass compositions with BaO content $\geq$ 40 mol% showed sharper exothermic peaks. The change of T_g (corresponding to a shift on the base line),and of T_c and T_p (these corresponding to the first exothermic peak) with the BaO content is presented in Fig. 4. It is observed that all these temperatures decrease with the substitution of BaO for ZnO. This means that Ba ions occupy network modifier positions together with Zn ions and that they have a stronger effect on the glass network disruption and decrease of rigidity compared with Zn ions. The temperature gap [T_c–T_g] corresponds to the interval in which structural rearrangements are allowed without the occurrence of crystallization. This range of temperatures is of major technological importance as it determines the so-called "working window" in which densification is expected to happen without devitrification. As shown in Fig. 4 the working window for the studied BaZBS compositions lies within a same interval of ~70°C, which is also an indication that their stability is quite similar.

The optimum sintering temperature (T_s), obtained from the bulk density measurement (which data will be shown in Fig. 5), and considered as the temperature at which the bulk density of a sintered glass sample reaches its highest value, is also shown in Fig. 4. It is verified that, for glasses with a BaO content $\leq$30 mol%, the beginning of crystallization occurs slightly after the end of the sintering process or maximum densification, i.e., $T_c > T_s$, whereas for glasses with higher BaO content, crystallization starts before the maximum density is attained i.e., $T_c < T_s$. These results indicate that sintering and crystallization happen as independent and sequential processes for glasses where substitution of BaO for ZnO was up to 30 mol%, but that for higher substitution levels, the crystallization process starts before complete densification hindering further sintering. As a consequence, sintered samples from glasses with BaO contents $\leq$30 mol%, are likely to keep their amorphous structure, whereas sintered samples from glasses with BaO >30 mol%, are prone to exhibit the presence of crystalline phases.

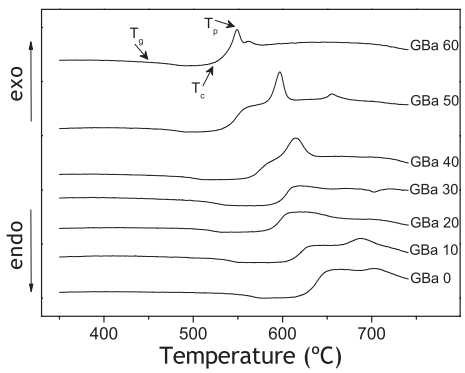

Fig. 3. DTA curves of glass powders obtained at a heating rate of 10°C/min.

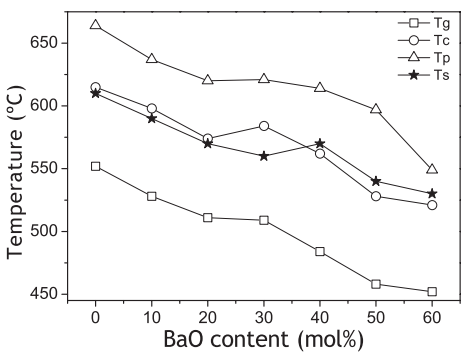

Fig. 4. Change of glass transition temperature (T_g), onset crystallization temperature (T_c), maximum crystallization temperature (T_p) and temperature of maximum densification (T_s) with BaO content.

(2) Sintering Behavior of the Glass Powders

The sintering behavior of the glass powders was studied by measurements of the density, porosity, and linear shrinkage of the powder compacts. For the different studied BaZBS glass compositions, the mean values of the bulk density after sintering at the various temperatures (ρ_s) were in the range 2.50–4.20 g/cm^3. To compare the effect of the sintering temperature on the densification of the various glass compositions, the relative increase in density, $D = (\rho_s - \rho_g)/\rho_g$, was calculated, which is dimensionless. Figure 5 shows the relative increase in density, D, as a function of the sintering temperature for the various BaZBS glass compositions. The variation of the apparent porosity with the sintering temperature is presented in Fig. 6 and linear shrinkage as a function of sintering temperature is presented in Fig. 7.

Although it is verified that the sintering of BaZBS glass powders is to a large degree temperature-dependent, it is clearly evident that the sintering behavior differs widely within the studied BaO compositional range. It is observed that the substitution of BaO for ZnO causes a decrease in

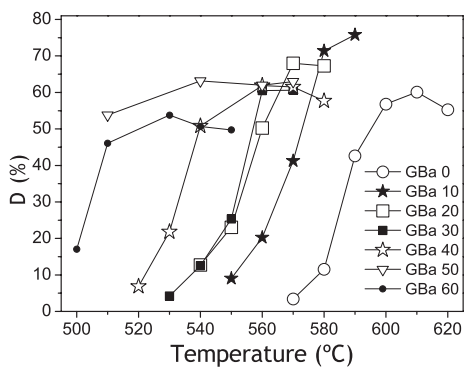

Fig. 5. Density increment as a function of sintering temperature for the different glass compositions.

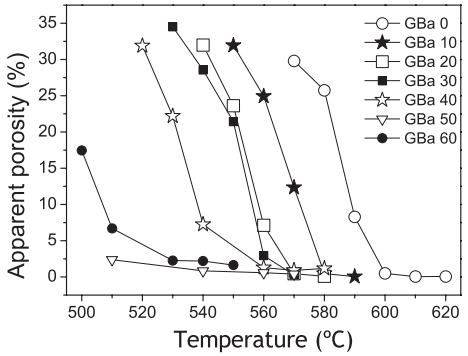

Fig. 6. Apparent porosity as a function of sintering temperature for the different glass compositions.

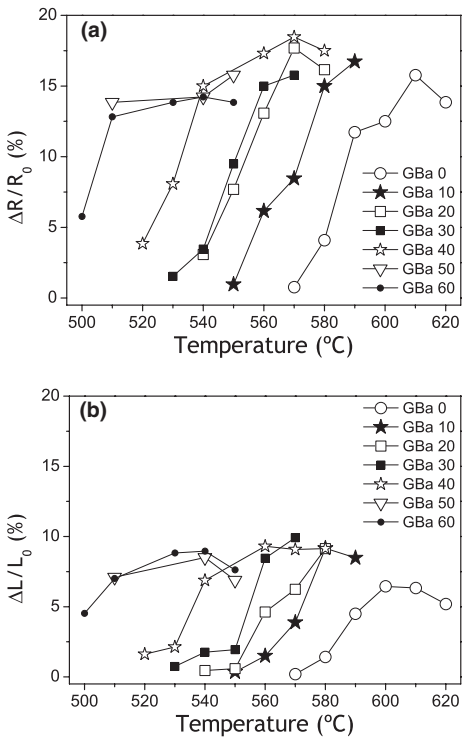

Fig. 7. Radial (a) and axial (b) shrinkage as a function of sintering temperature for the different glass compositions.

the temperature where the density starts rising (Fig. 5), i.e., porosity starts falling (Fig. 6). For example, for GBa0, D starts to increase at 570°C reaches a maximum at 610°C and then it slightly decreases, whereas for GBa10, D starts to increase sharply at 550°C and reaches a maximum at 590°C, and for GBa50, the value for D at 510°C is comparatively higher than for the other samples treated at this temperature, but it reaches a maximum at 530°C and then stays nearly constant.

Samples with a BaO content ≤ 30 mol%, when sintered at the temperature where maximum densification is achieved (T_s), reached an apparent porosity equal to zero (see Fig. 6), indicating that all open porosity had disappeared and that only isolated closed pores remained in the sintered samples. For those samples, the slight decrease in density at the highest sintering temperature is due to the so-called over-firing phenomenon, Park *et al.*[20] quoted in Kim *et al.*,[4] which has also been found in different samples made from the ternary systems Bi_2O_3–B_2O_3–SiO_2[4] and BaO–B_2O_3–SiO_2.[10] Samples with 40 mol% BaO, or higher content, exhibited almost a density plateau above T_s (see Fig. 5), and the corresponding apparent porosity attained a minimum value (<1.5%), as seen in Fig. 6. The evolution of the linear shrinkage with sintering temperature (Fig. 7) is similar to that of the densification (Fig. 5), as expected. However, it is observed that the values of radial shrinkage, Fig. 7(a), are higher than those of axial shrinkage Fig. 7(b) (same ordinate scale), meaning that the glass samples exhibit anisotropic shrinkage during sintering.

In a simple way, the process of sintering of a glass can be considered as the heat treatment that causes the grains to adhere to each other.[17] Sintering of a glass powder occurs by the viscous flow mechanism[16] and the initial rate of sintering of glass powders is inversely proportional to the viscosity of the glass.[17,21] Ba^{2+} ions have a stronger effect on the decrease of the rigidity of the glass network compared to Zn^{2+} (as inferred by the T_g values, Fig. 4). In fact, the cation field strength Z/r^2 (where Z is the valence number and r the ionic radius) is 0.99 for Ba^{2+} and 5.56 for Zn^{2+},[22] meaning that the structural deformability is enhanced by the presence of Ba^{2+}. Thus, the higher the BaO content, the lower the temperature where densification starts (as seen in Fig. 5). However, for glass samples with high BaO levels (>40 mol%), the crystallization process starts before the end of the sintering process ($T_c < T_s$, Fig. 4), and further densification/shrinkage is hindered, as illustrated in Figs. 5 and 7, which show that for those samples the density/shrinkage values were nearly constant at the highest sintering temperatures.

When a powdered glass is heat-treated, before crystallization begins, the sintering process is due to the viscous flow of initial glass, but if at a certain stage, crystallization starts, this is accompanied by a decrease in the amount of the glassy phase and an increase in the materials viscosity. As a result, the rate of sintering, which proceeds at the cost of viscous flow, decreases.[17]

The XRD patterns of the BaZBS glass samples sintered at various temperatures are shown in Fig. 8. Samples with a BaO content ≤ 30 mol%, sintered at temperatures within the working window(500°C–610°C)were amorphous, cf. Fig. 8(a), agreeing with the fact that the end of sintering occurred before crystallization. This was observed for the studied glasses where substitution of BaO for ZnO was up to 30 mol%. For sintered GBa0 ($60ZnO$–$30B_2O_3$–$10SiO_2$), a broad peak appears around $2\theta = 35°$, Fig. 8(a), similar to that observed in the XRD pattern prior to sintering, Fig. 1. XRD patterns obtained for different glasses with a composition (60–66)ZnO –(14–15)B_2O_3–(20–25)SiO_2 revealed that the amorphous structure was retained even after heat treating bulk samples for 3 h at 650°C,[23] 775°C[24], and 745°C.[25] XRD patterns for sintered BaZBS glasses, with a BaO content 10–30 mol%, show a broad peak around $2\theta = 28°$, Fig. 8(a), as observed in the XRD patterns prior to sintering, Fig. 1.

XRD patterns obtained for GBa40, Fig. 8(b), indicate that samples are still amorphous when treated at 520°C (below T_c), but that crystalline phases, such as barium zinc silicate ($BaZnSiO_4$) and barium borate (BaB_4O_7), are present after sintering at 570°C (T_s). For GBa50, Fig. 8(c), treated at 510°C (below T_c), the presence of barium zinc silicate and barium silicate ($Ba_5Si_8O_{21}$) was identified, and an additional phase, beta barium borate (β-BaB_2O_4), was identified in samples sintered at 570°C. For GBa60, with full substitution of ZnO, beta barium borate was present in samples treated at 500°C (below T_c) and an extra phase, barium silicate, was identified in samples sintered at 560°C, Fig. 8(d). These results indicate that for the higher substitution levels, the crystallization process starts before complete densification at temperatures much lower than those indicated by the DTA plots (T_c), hindering further sintering. A much lower densification was evident for GBa60 comparatively to the other samples (see Fig. 5), which was caused by early crystallization before densification was initiated.

Figure 9 shows fracture surface SEM images of sintered BaZBS glasses. Figures 9(a)–(c) correspond to the microstructures of GBa0, GBa10, and GBa20, respectively, and in

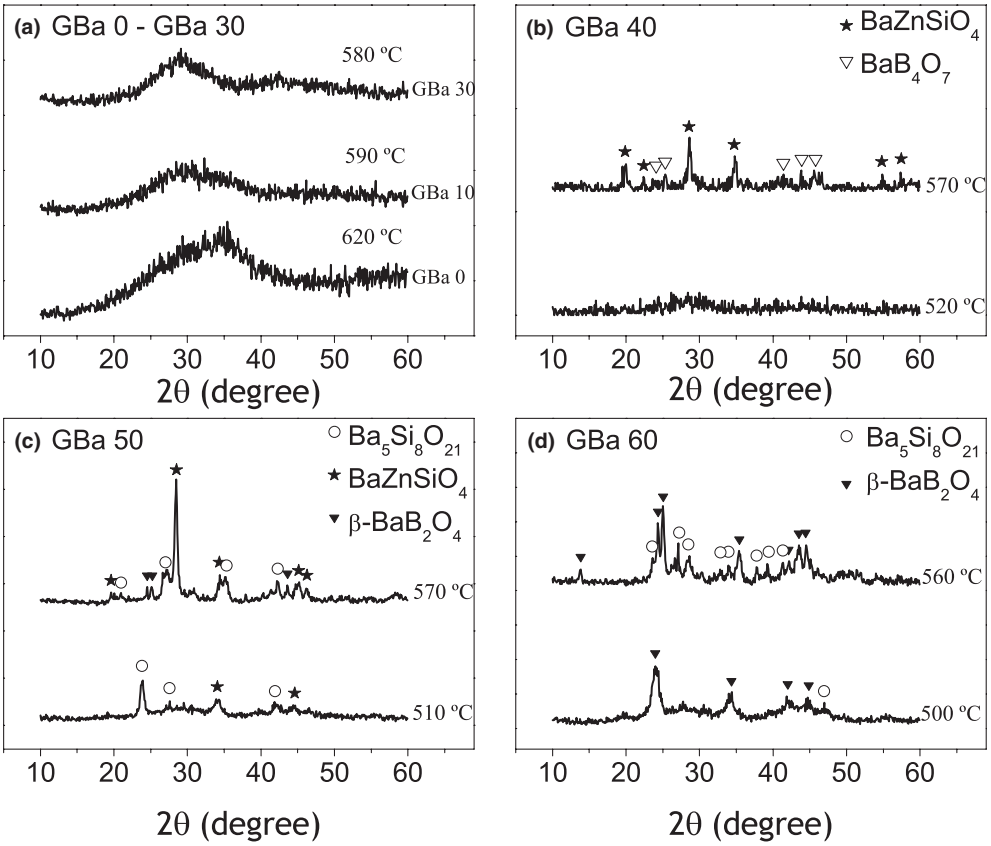

Fig. 8. XRD patterns of the glass samples sintered at various temperatures.

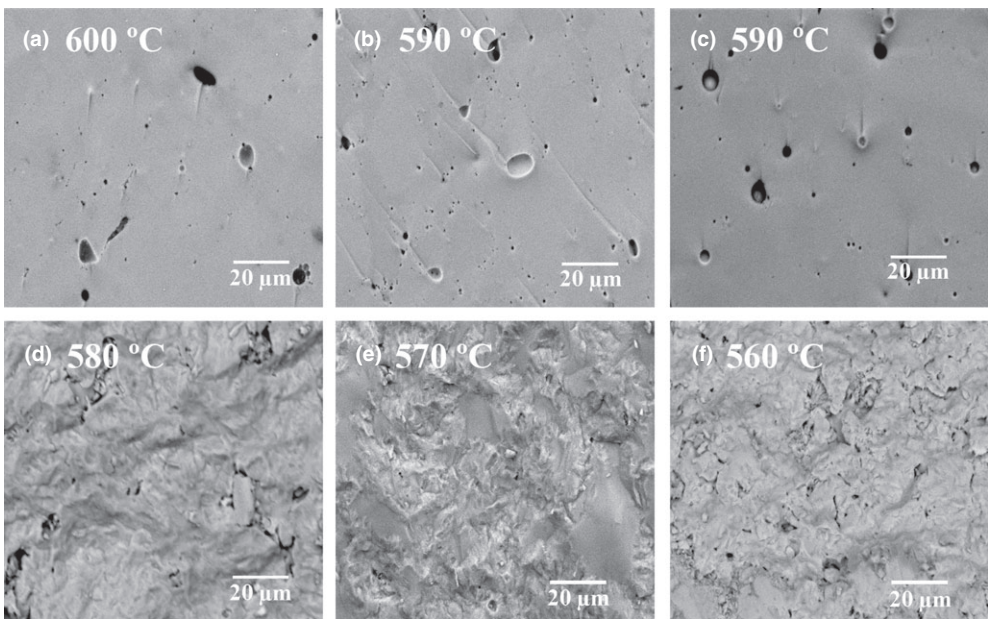

Fig. 9. SEM photographs of GBa0 (a), GBa10 (b), GBa20 (c), GBa40 (d), GBa50 (e), and GBa60 (f), sintered at selected temperatures.

every sample a well-densified glass is observed that did not crystallize during the whole sintering process. Some closed pores within a smooth fracture surface, which is a typical feature of glass, can be observed after sintering. Figures 9(d)–(f) correspond to the microstructures of samples GBa40, GBa50, and GBa60, respectively. Rough surfaces are observed due to the crystallized phases that were formed during the heat treatment of the glasses and some closed pores are visible. Data for closed porosity of sintered BaZBS glasses will be shown in Table II.

(3) Dielectric Characterization

The results from the measurements of the dielectric properties of the sintered BaZBS glasses (dielectric constant, ε_r, and loss tan δ over three different frequencies) are presented in Table II, which shows also the sintering temperature and closed porosity of the specimens. It is observed that ε_r values increased as BaO content increased and, as for the frequency effect, no significant difference was detected, although slightly higher ε_r values were determined at relatively lower frequencies.

Table II. Dielectric Constant, ε, and Loss Tang (tan δ) for Sintered BZBS Glass Samples at Different Frequencies. Sintering Temperature and Closed Porosity are shown

Glass	Sintering temperature (°C)	Closed porosity (%)	100 kHz	500 kHz	1 MHz
GBa0	600	8	7.70 (0.005)	7.71 (0.006)	7.69 (0.004)
GBa10	590	8	8.78 (0.003)	8.75 (0.003)	8.74 (0.002)
GBa20	580	3	9.63 (0.002)	9.60 (0.002)	9.59 (0.002)
GBa30	570	2	10.45 (0.003)	10.42 (0.003)	10.41 (0.004)
GBa40	570	2	9.68 (0.004)	9.63 (0.005)	9.61 (0.006)
GBa50	550	5	10.24 (0.009)	10.15 (0.008)	10.11 (0.008)
GBa60	550	10	10.87 (0.056)	10.41 (0.033)	10.29 (0.024)

The increase in dielectric constant with BaO is attributed to the fact that the polarizability of Ba^{2+} ion is greater than that of Zn^{2+} ion, the ionic size being Ba^{2+} = 1.42 Å and Zn^{2+} = 0.75 Å,[26] and the cation field strength 0.99 for Ba^{2+} and 5.56 for Zn^{2+}.[22] In fact, for glasses from the ternary systems $BaO–B_2O_3–SiO_2$ and $ZnO–B_2O_3–SiO_2$, it was verified that an increase in modifying oxide(BaO and ZnO) raises the dielectric constant of the glasses and that BaO was more effective in raising the dielectric constant than ZnO.[27]

Our ε_r values measured at 1 MHz were compared with those measured at the same frequency on sintered glasses from the ternary system $BaO–B_2O_3–SiO_2$ (BaBS).[3,6] It was observed that for a BaO content of 20 mol%, ε_r obtained for BaZBS glass (9.59) was higher than for BaBS glass (7.39),[3] whereas for BaO $\geq$ 40 mol%, ε_r values (9.61–10.29) obtained for the sintered BaZBS glasses investigated in the present study were lower than those reported for BaBS glasses (10.3–11.7).[6]

The dielectric constant of the BaZBS glasses was calculated theoretically on the basis of the model described by Appen and Breska quoted in Ref. 28 According to this empirical model, $\varepsilon_r = 10^{-2}\Sigma\varepsilon_{ri}\rho_i$, where ρ_i is the amount of individual oxides (in mol%) and ε_{ri} the characteristic factor for each oxide: BaO is 20.5, ZnO is 14.4, B_2O_3 is 3–8, and SiO_2 is 3.8. As the factor value of B_2O_3 has upper and lower limits, which depend upon glass composition,[28] a theoretical range of ε_r was determined for the glass compositions investigated in this study. Figure 10 shows that the whole set of experimental values of ε_r were much lower than the values calculated according to the model described by Appen and Breska.[28]

The discrepancy between the calculated and experimental results may have arisen from a rough estimation of the provided dielectric constant factor ε_{ri} of the model and, mainly, because it was predicted for bulk glasses, i.e., without any porosity. It has been reported that this estimation was dependent on the type of glass system and the number of constituents in the system, i.e., binary, ternary, or quaternary system.[9,29]

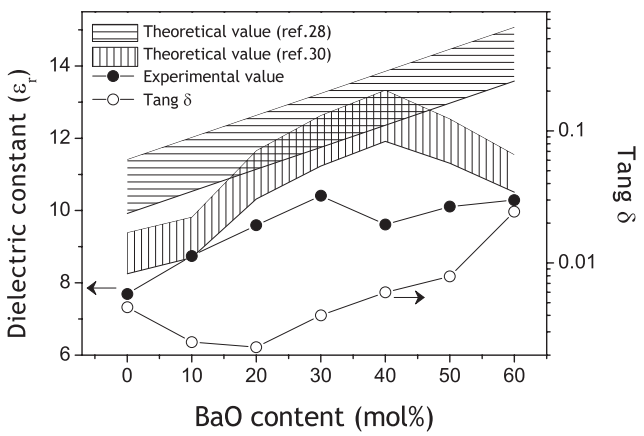

Fig. 10. Dielectric constant (ε_r) and tan δ as a function of BaO content (at 1 MHz), and comparison of ε_r experimental data with theoretical data.

To take into account the effect of closed porosity on the dielectric constant of the sintered BaZBS glasses, an empirical equation for the calculation of the dielectric constant of a mixture was considered[30]: $\epsilon_r^n = \vartheta_1\epsilon_{r1}^n + \vartheta_2\epsilon_{r2}^n$, ϑ_1 and ϑ_2 are the volume fraction of the glass and of the closed pores, respectively, ϵ_{r1}^n and $\epsilon_{r2}^n$are the dielectric constant of the glass and of the pores, respectively, and n is a constant. The value of the constant determines the type of mixing rule[30]: $n = -1$ (serial mixing model), $n = 1$ (parallel mixing model), and $n = 0$ (logarithmic mixing model). The volume fraction of the glass and of the closed pores (Table II), the dielectric constant of the glass (calculated according to the composition on the basis of Appen and Breska's equation),[28] and the dielectric constant of the pores (equal to 1) have been considered for calculation, and it was verified that the values calculated by the logarithmic mixing rule[30] adjusted better to the experimental ε_r values (see Fig. 10). However, the experimental values were smaller than the predicted values, this being particularly observed in the compositional range BaO $\geq$ 40 mol%, where some crystalline phases are present in unknown amount and were not considered in the calculation. It is believed that the formation during sintering of some of these crystalline phases, for instance BaB_2O_4 (cf. Fig. 8), with ε_r in the range 5–8,[10] will lower the resultant dielectric constant of the sintered BaZBS glass.

It should be noted that the value of dielectric loss for the generality of these materials is quite low (i.e., of the order of 10^{-3}) except for the higher molar volume fraction used. This indicates these materials to be both good insulators as well as having low dielectric heating properties.

IV. Conclusions

The present study investigated the effect of BaO substitution for ZnO on the sintering and crystallization behavior of Pb-free low-temperature firing $BaO–ZnO-B_2O_3–SiO_2$ glasses. Both T_g and T_c decreased as the relative amount of BaO increased. Depending on the level of BaO substitution for ZnO, different sintering behaviors of the glasses were observed. When T_c was higher than T_s, the sample was well-densified at T_s, and a fully amorphous material was obtained, as in the case of glasses with BaO $\leq$ 30 mol%. When T_s was higher than T_c, crystallization and densification progressed at the same time, and the presence of the crystalline phases inhibited densification, as in the case of glasses with BaO $\geq$ 40 mol%. Substitution of BaO for ZnO caused an increase in the dielectric constant of the sintered glasses.

Acknowledgments

This work was financially supported by the Portuguese Foundation for Science and Technology through Project PTDC/CTM/102141/2008, and funding to CENIMAT/I3N (Strategic Project PEst-C/CTM/LA0025/2011) and to CICECO (Center for Research in Ceramic and Composite Materials, University of Aveiro).

References

[1]Z. Wang, Y. Hu, H. Lu, and F. Yu, "Dielectric Properties and Crystalline Characteristics of Borosilicate Glasses," *J. Non-Cryst. Solids*, **354**, 1128–32 (2008).

[2]N. Santha, S. Shamsudeen, N. T. Karunakaran, and J. I. Naseemabeevi, "Spectroscopic, Dielectric and Optical Properties of $60ZnO–30B_2O_3–10SiO_2$ Glass–Al_2O_3 Composites," *Int. J. Appl. Ceram. Technol.*, **8**, 1042–9 (2011).

[3]E.-S. Lim, B.-S. Kim, J.-H. Lee, and J.-J. Kim, "Characterization of the Low Temperature Firing $BaO-B_2O_3-SiO_2$ Glass: The Effect of BaO Content," *J. Eur. Ceram. Soc.*, **27**, 825–9 (2007).

[4]B.-S. Kim, E.-S. Lim, J.-H. Lee, and J.-J. Kim, "Effect of Bi_2O_3 Content on Sintering and Crystallization Behavior of Low-Temperature Firing $Bi_2O_3–B_2O_3–SiO_2$ Glasses," *J. Eur. Ceram. Soc.*, **27**, 819–24 (2007).

[5]M. J. Pascual, A. Duran, and L. Pascual, "Sintering Process of Glasses in the System $Na_2O–B_2O_3–SiO_2$," *J. Non-Cryst. Solids*, **306**, 58–69 (2002).

[6]E.-S. Lim, B.-S. Kim, J.-H. Lee, and J.-J. Kim, "Effect of BaO Content on Sintering and Physical Properties of $BaO-B_2O_3-SiO_2$ Glasses," *J. Non-Cryst. Solids*, **352**, 821–6 (2006).

[7]G. H. Hwang, H. J. Jeon, and Y. S. Kim, "Physical Propeties of Barrier Ribs of Plasma Display Panels: I. Formation of Pores During Sintering of Lead Borosilicate Glass Frits," *J. Am. Ceram. Soc.*, **85**, 2956–60 (2002).

[8]G. H. Hwang, W. Y. Kim, H. J. Jeon, and Y. S. Kim, "Physical Properties of Barrier Ribs of Plasma Display Panels. Part II. Effects of Fillers," *J. Am. Ceram. Soc.*, **85**, 2961–4 (2002).

[9]S.-G. Kim, H. Shi, J.-S. Park, K. S. Hong, and H. Kim, "Effect of SiO_2 Addition to $BaO-ZnO-B_2O_3$ Glass on Dielectric and Thermal Properties for Application to Barrier Ribs of Plasma Display Panels," *J. Electroceram.*, **15**, 129–34 (2005).

[10]E.-S. Lim, B.-S. Kim, J.-H. Lee, and J.-J. Kim, "Dielectric, Thermal and Sintering Behaviour of $BaO-B_2O_3-SiO_2$ Glasses with the Addition of Al_2O_3," *J. Electroceram.*, **17**, 359–64 (2006).

[11]D. N. Kim, J. Y. Lee, J. S. Huh, and H. S. Kim, "Thermal and Electrical Properties of $BaO-B_2O_3$-ZnO Glasses," *J. Non-Cryst. Solids*, **306**, 70–5 (2002).

[12]C. L. Yaws, *Chemical Properties Handbook: Physical, Thermodynamic, Environmental, Transport, Safety and Health Related Properties for Organic and Inorganic Chemicals*, pp. 613–5, McGraw-Hill Book Co, New York, 1999.

[13]S.-G. Kim, J.-S. Park, J.-S. An, K. S. Hong, H. Shin, and H. S. Kim, "Effect of the Addition of Different Types of Fillers in the Properties of $BaO-ZnO-B_2O_3-SiO_2$ Glass Composites for Application to Barrier Ribs of Plasma Display Panels," *J. Am. Ceram. Soc.*, **89**, 902–7 (2006).

[14]D. S. Jung, S. K. Hong, J. S. Cho, and Y. C. Kang, "Spherical Shape $BaO-ZnO-B_2O_3-SiO_2$ Glass Powders Prepared by Spray Pyrolysis," *Appl. Phys. A*, **89**, 769–74 (2007).

[15]H. Shin, S.-G. Kim, J.-S. Park, J.-S. An, K. S. Hong, and H. Kim, "Co-Additions of TiO_2 and SiO_2 Crystalline Fillers to Tailor the Properties of $BaO–ZnO–B_2O_3–SiO_2$ Glass for Application to Barrier Ribs of Plasma Display Panels," *J. Am. Ceram. Soc.*, **89** [10] 3258–61 (2006).

[16]G. Kuczynski, "Study of Sintering of Glass," *J. Appl. Phys.*, **20**, 1160–3 (1949).

[17]A. E. Shilo, E. K. Bondarev, and S. A. Kukharenko, "Sintering of Low-Melting Glass Powders and Glass-Abrasive Composites," *Sci. Sinter.*, **35**, 117–24 (2003).

[18]M. M. Lima and R. C. C. Monteiro, "Characterization and Thermal Behavior of a Borosilicate Glass," *Thermochim. Acta*, **373**, 69–74 (2001).

[19]B.-M. J. Snyder, M. G. Mesko, and J. E. Shelby, "Volatilization of Boron from E-glass Melts," *J. Non-Cryst. Solids*, **352**, 669–73 (2006).

[20]D. H. Park, B. C. Kim, J. J. Kim, and L. S. Park, "Effect of Glassparticle Size on Sintering Behaviors of the Glass–Alumina Composites for Low Firing Temperature," *J. Korean Ceram. Soc.*, **37**, 545–51 (2000).

[21]D. Kingery and M. Berg, "Studies of Initial Stages of Sintering Solid by Viscous Flow, Evaporation – Condensation and Sell-Diffusion," *J. Appl. Phys.*, **26**, 1205–6 (1955).

[22]S. Toyoda, S. Fujino, and K. Morinaga, "Density, Viscosity and Surface Tension of $50RO–50P_2O_5$(R: Mg, Ca, Sr, Ba, and Zn)Glass Melts," *J. Non-Cryst. Solids*, **321**, 169–74 (2003).

[23]Z. Khalkhali, Z. Hamnabard, S. S. A. Qazvini, S. Baghshahi, and A. Maghsoudipour, "Preparation, Phase Formation and Photoluminescence Properties of $ZnO–SiO_2–B_2O_3$ Glasses with Different ZnO/B_2O_3 Ratios," *Opt. Mater.*, **34**, 850–5 (2012).

[24]S. S. A. Qazvini, Z. Hamnabard, Z. Khalkhali, S. Baghshahi, and A. Maghsoudipour, "Photoluminescence and Microstructural Properties of $SiO_2–ZnO–B_2O_3$ System Containing TiO_2 and V_2O_5," *Ceram. Int.*, **38**, 1663–70 (2012).

[25]Z. Hamnabard, Z. Khalkhali, S. S. A. Qazvini, S. Baghshahi, and A. Maghsoudipour, "Preparation, Heat Treatment and Photoluminescence Properties of V-Doped $ZnO–SiO_2–B_2O_3$ Glasses," *J. Lumin.*, **132**, 1126–32 (2012).

[26]B. H. Jung, D. K. Lee, S. H. Sohn, and H. S. Kim, "Thermal, Dielectric, and Optical Properties of Neodymium Borosilicate Glasses for Thick Films," *J. Am. Ceram. Soc.*, **86**, 1202–4 (2003).

[27]J.-M. Wu and H.-L. Huang, "Microwave Properties of Zinc, Barium and Lead Borosilicate Glasses," *J. Non-Cryst. Solids*, **260**, 116–24 (1999).

[28]H. Scholze, *Glass, Nature, Structure, and Properties* (translated by Michael J. Lakin), 3rd edition, Springer–Verlag, New York, 1991.

[29]G.-H. Hwang, W.-Y. Kim, H.-J. Jeon, and Y.-S. Kim, "Physical Properties of Barrier Ribs of Plasma Display Panels: II, Effects of Fillers," *J. Am. Ceram. Soc.*, **85**, 2961–4 (2002).

[30]W. D. Kingery, H. K. Bowen, and D. R. Uhlmann, *Introduction to Ceramics*. 2nd edition, pp. 947–8, John Wiley & Sons, New York, 1976. □